JOURNAL OF THERMOPHYSICS AND HEAT TRANSFER
Vol. 23, No. 4, October–December 2009

Rate Parameters for Electronic Excitation of Diatomic Molecules: NO Radiation

Seong-Yoon Hyun,* Chul Park,† and Keun-Shik Chang‡
Korea Advanced Institute of Science and Technology, Daejeon 305-701, Republic of Korea

DOI: 10.2514/1.42686

This is one of an ongoing series of papers on collisional excitation of electronic states in N_2, O_2, NO, CO, CN, and N_2^+. In this paper, NO radiation observed in the test section of an arcjet wind tunnel is studied. In the experiments, NO γ and δ were seen, β was not seen, and ε was seen to be very weak. NO radiation is calculated with the use of the code SPRADIAN07 to explain the measured spectra. It was found that inverse predissociation is mainly responsible for the population of the NO $C^2\Pi_r$ state during recombination of N and O atoms. The population of the NO $A^2\Sigma^+$ state is mostly due to the radiative decay from the NO $C^2\Pi_r$ state. The NO $D^2\Sigma^+$ state is excited from the $C^2\Pi_r$ state by collisions. The NO $B^2\Pi_r$ state is populated by complicated collisional transition paths by passing through the intermediate states $a^4\Pi_r$ and $b^4\Sigma^-$. These interpretations at least qualitatively explain the experimental data. Electronic excitation temperature is only remotely related to electron temperature.

Nomenclature

A = electronic state of the NO molecule, $A^2\Sigma^+$
A_h = excitation rate parameter, $\mathrm{cm^3/s}$
A_r = radiative transition probability, $\mathrm{s^{-1}}$
a = electronic state of the NO molecule, $a^4\Pi$
B = electronic state of the NO molecule, $B^2\Pi_r$
b = electronic state of the NO molecule, $b^4\Sigma^-$
C = electronic state of the NO molecule, $C^2\Pi_r$
D = electronic state of the NO molecule, $D^2\Sigma^+$
E = electronic term energy, $\mathrm{cm^{-1}}$; energy, $\mathrm{cm^{-1}}$
g = statistical weight (multiplicity, degeneracy)
h = Plank constant, $6.6261 \times 10^{-34}\ \mathrm{J \cdot s}$
I = total band intensity, $\mathrm{W/(cm^3)}$
I_λ = specific intensity, $\mathrm{W/(cm^2 \cdot \mu m \cdot sr)}$
i = electronic state i of the NO molecule
J = rotational quantum number; rotational state
j = electronic state j of the NO molecule
K_e = excitation rate by electron collision, $\mathrm{cm^3/s}$
K_h = excitation rate by heavy-particle collision, $\mathrm{cm^3/s}$
K_{ivpr} = rate coefficient for inverse predissociation, $\mathrm{cm^3/s}$
K_{prd} = rate coefficient for predissociation, $\mathrm{s^{-1}}$
k_B = Boltzmann constant, $1.3807 \times 10^{-23}\ \mathrm{J/K}$
k_λ = absorption coefficient, $\mathrm{cm^{-1}}$
M = colliding heavy particle or electron
m = mass, g/mol
n = number density, $\mathrm{cm^{-3}}$; excitation rate parameter, Eq. (10)
p = pressure, atm
Q = partition function
S = spin angular momentum quantum number
$S_{J''\Lambda''}^{J'\Lambda'}$ = rotational line strength factor (Hönl–London factor)
s = distance along a ray, cm
T = heavy-particle translational temperature, K
T_d = activation temperature, K
T_e = electron temperature, K
T_{ex} = electronic excitation temperature, K
T_r = heavy-particle rotational temperature, K
T_v = vibrational temperature, K
t = time, s
v = vibrational quantum number, vibrational state
X = ground electronic state of the NO molecule, $X^2\Pi_r$
x = distance from the nozzle exit
β = NO $B^2\Pi_r - X^2\Pi_r$ transition
γ = NO $A^2\Sigma^+ - X^2\Pi_r$ transition
δ = NO $C^2\Pi_r - X^2\Pi_r$ transition
δ_K = Kronecker delta
ε = NO $D^2\Sigma^+ - X^2\Pi_r$ transition
ε_λ = emission coefficient, $\mathrm{W/(cm^2 \cdot \mu m \cdot sr)}$
κ = nonequilibrium factor
λ = wavelength, Å or nm
Λ = orbital angular momentum quantum number about the internuclear axis
ν = frequency, Hz
σ = cross section, $\mathrm{cm^2}$
χ = total mole fraction

Subscripts

A = electronic state of the NO molecule, $A^2\Sigma^+$
a = electronic state of the NO molecule, $a^4\Pi$
B = electronic state of the NO molecule, $B^2\Pi_r$
b = electronic state of the NO molecule, $b^4\Sigma^-$
C = electronic state of the NO molecule, $C^2\Pi_r$
D = electronic state of the NO molecule, $D^2\Sigma^+$
e = electron
eq = under Boltzmann distribution
h = heavy particle
i = electronic state i of an atom or molecule
nq = under non-Boltzmann distribution
t = total
X = ground electronic state of an atom or molecule

Superscripts

$'$ = upper state
$''$ = lower state

I. Introduction

ARCJET wind-tunnel facilities have been used to test thermal protection materials. Arcjet nozzle flows have been known to be in thermal and chemical nonequilibrium. Many experimental and theoretical efforts have been made to characterize such flows.

Received 11 December 2008; accepted for publication 25 May 2009.

*Postdoctoral Researcher, Department of Aerospace Engineering; heinne@kaist.ac.kr. Student Member AIAA.

†Professor, Department of Aerospace Engineering. Fellow AIAA.

‡Professor, Department of Aerospace Engineering. Member AIAA.

Table 1 Experimental conditions and temperatures taken from Babikian et al. [2] and Park et al. [7,8]

	Babikian et al. [2]		Park et al. [7,8]	
	Flow solution	Measured	Measured (1998)	Measured (1999)
λ, Å	——	$2,250 < \lambda < 3,050$	$2,000 < \lambda < 2,800$	
x, cm	——	35.6	34.5	30
Temperatures, K				
T	560	——	——	820 ± 250, $1,640 \pm 400$
T_r	560	560 ± 50	$850 < T_r < 950$	$600 < T_r < 1,000$
T_v(NO)	950	950 ± 50	≥ 950	≤ 950
T_e	6,100	——	——	——
T_{ex}	——	$11,500 \pm 520$	$12,950 \pm 800$	——

Park and Lee [1] developed a multitemperature nozzle flow code. It was used to determine rotational, vibrational, and electron–electronic temperatures by Park and Lee [1] and Babikian et al. [2] of NASA Ames Research Center. They assumed that heavy-particle translational temperature is equal to rotational temperature, and vibrational temperatures of NO, N_2, and O_2 are different from each other. Abe et al. [3] of Kyushu University introduced eight temperatures to characterize arc-heated nozzle flows: that is, translational, N_2-, O_2-, and NO-rotational; N_2-, O_2-, and NO-vibrational; and electron temperatures.

In experimental studies, spectra from NO molecule have been measured to characterize flows. NO has many radiative transition band systems [4–6]. Important among them are NO $\gamma(A^2\Sigma^+ - X^2\Pi_r)$, $\beta(B^2\Pi_r - X^2\Pi_r)$, δ $(C^2\Pi_r - X^2\Pi_r)$, and ε $(D^2\Sigma^+ - X^2\Pi_r)$. In 1994, Babikian et al. [2] reported uncalibrated NO spectra measured in an arcjet facility, named the Aerodynamic Heating Facility, in NASA Ames Research Center. They deduced rotational, NO-vibrational, and electronic excitation temperatures from the obtained spectra. The measured temperatures were $T_r = 560$, $T_v(\mathrm{NO}) = 950$, and $T_{\mathrm{ex}} = 11,500$ K. In 1998 and 1999, Park et al. [7,8] of NASA Ames Research Center also reported calibrated NO spectra measured in the same facility. The spectra [7] taken at 34.5 cm from the nozzle exit in 1998 have exactly the same shape as the spectra [8] obtained at 30 cm from the nozzle exit in 1999. They also determined such temperatures by analyzing the obtained spectra. The measured temperatures shown in the consecutive reports were T_r within the ranges of 600 to 1000, $T_v(\mathrm{NO}) \simeq 950$, and $T_{\mathrm{ex}} = 12,950$ K.

Babikian et al. [2] performed flowfield computations and obtained $T = T_r = 560$, $T_v(\mathrm{NO}) = 950$, and $T_e = 6100$ K. The measured rotational and NO-vibrational temperatures showed fairly good agreement with the temperatures determined in the flow calculation. The spectra of NO γ and δ band systems calculated under the assumption of Boltzmann excitation almost fit the measured data. But there are still unanswered questions about the measured temperatures and the measured NO spectra. The electron temperature determined in the flow computation ($T_e = 6100$ K) is very different from the electronic excitation temperature deduced from the experiment ($T_{\mathrm{ex}} = 11,500$ K): T_e is generally accepted to be the same as T_{ex} because electronic excitation occurs very efficiently by electron collisions. The observed $T_e \neq T_{\mathrm{ex}}$ defies this assumption.

The NO spectra calculated by Babikian et al. [2] showed the spectrum of NO β band system that was not seen in the measured data. In the measurement of Park et al. [7,8], NO ε radiation was expected to be strong at wavelengths shorter than 2200 Å if the NO $D^2\Sigma^+$ state was populated under the Boltzmann distribution. But such strong ε radiation was not found in the measured spectra. These abnormal phenomena of NO β and ε in the arcjet flows were often simply attributed to non-Boltzmann excitations of NO electronic states [2,7,8]. But detailed excitation mechanisms have not been systematically investigated. Abe et al. [3] also measured NO spectra in an arc-heated wind tunnel in Kyushu University. The obtained spectra, which was not calibrated, showed intense vibrational bands of NO $\gamma(v' = 0\text{–}3)$ and $\delta(v' = 0)$ in the wavelengths of 2200 to 2650 Å. The existence of the β and ε band systems could not be confirmed.

This is one of an ongoing series of papers [9–12] on collisional excitation of electronic states in N_2, O_2, NO, CO, CN, and N_2^+. The purpose of this series is to verify the accuracy of the SPRADIAN07 [9–14] and the input data through computations of NO radiation under both Boltzmann and supposedly non-Boltzmann excitations. Boltzmann calculations for the spectra of NO γ, β, δ, and ε are numerically performed with the use of the SPRADIAN07. The code assumes that a quasi-steady-state (QSS) condition [13–15] exists among internal electronic states to calculate non-Boltzmann radiation. Non-Boltzmann radiation was indirectly computed because of the following:

1) The states of NO $C^2\Pi_r$ and $D^2\Sigma^+$ and their collisional excitation rates are presently not available in the code.

2) The excitation mechanisms were found to be very different from collisional process.

Collisional transition rates for available transitions are estimated by the code.

The present work tries to qualitatively explain the excitation mechanisms of NO electronic states for the data obtained by the two groups [2,7,8] of NASA Ames Research Center. Inverse predissociation phenomena, sometimes referred to as preassociation or chemiluminescence, are introduced to do so. The effects of collisional and radiative transitions are also qualitatively discussed.

II. Available Data

A. Flowfield

The temperatures and species number densities determined by Babikian et al. [2] in the flow solution are tabulated in Tables 1 and 2. They are the values at the point at which the experimental measurements were made. The species number densities can contain uncertainties because they were read from the figures in the work of Babikian et al.

As mentioned, Babikian et al. [2] determined rotational, electronic excitation, and NO-vibrational temperatures by fitting the spectra computed with the used of the modified version [5] of NEQAIR85 [16] with the measured spectra. The measured temperatures are listed in Table 1. In both the work of Babikian et al. [2] and Park et al. [7,8], electronic excitation temperatures were determined by comparing the intensities of NO γ and δ bands. The temperatures determined in the flow solution are consistent with the measured temperatures except for electron temperature: $T_e = 6100$ K is significantly different from $T_{\mathrm{ex}} = 11,500$ K.

Flowfield data for the experiment of Park et al. [7,8] were not available, but the temperatures deduced by them from the measured

Table 2 Species number densities taken from Babikian et al. [2]

Number densities[a], cm^{-3}			
n_{N}	5.56×10^{15}	n_{O}	2.72×10^{15}
$n_{\mathrm{N_2}}$	2.41×10^{15}	$n_{\mathrm{O_2}}$	3.96×10^{12}
$n_{\mathrm{N^+}}$	4.10×10^{12}	$n_{\mathrm{O^+}}$	1.28×10^{12}
n_{NO}	2.41×10^{13}	$n_{\mathrm{E^-}}$	5.56×10^{12}

[a] At $p = 8.72 \times 10^{-4}$ atm and $T = 560$ K.

spectra were similar to those of Babikian et al. [2], as shown in Table 1. Heavy-particle translational temperatures [8] determined from the line widths were 820 and 1640 K at the settling chamber pressures of 1.72×10^5 and 6.88×10^5 Pa, respectively.

B. Radiation

NO spectra are produced with the use of the code SPRADIAN07 in the present work. The code solves the radiative transfer equation, $\mathrm{d}I_\lambda/\mathrm{d}s = \varepsilon_\lambda - k_\lambda I_\lambda$, along a line of sight by assuming that emission and absorption coefficients vary linearly between two given points. The emission and absorption coefficients ε_λ and k_λ are computed using the line-by-line technique in this code. Electronic-vibrational transition moments are taken from the works of Laux [5] and Laux and Knucinnt [17] for NO γ, β, δ, and ε band systems. The Hönl–London factors $S_{J''\Lambda''}^{J'\Lambda'}$ for $^2\Sigma - {}^2\Pi$ and $^2\Pi - {}^2\Pi$ transitions are formulated from Kovács [18] and corrected by the sum rule of [19–21]

$$\sum S_{J''\Lambda''}^{J'\Lambda'} = (2 - \delta_{K,(0,\Lambda'+\Lambda'')})(2S+1)(2J+1)$$

Spin-orbit coupling constants [5,13,22] are 123.3 cm^{-1} for $X^2\Pi_r$, 31.32 cm^{-1} for $B^2\Pi_r$, and 3.0 cm^{-1} for $C^2\Pi_r$. A more detailed description on diatomic bound–bound transition contained in the code can be found in [13,14].

As mentioned, spectral intensities for NO γ and δ band systems are computed under the Boltzmann excitation assumption. Those of NO β and ε are computed under the Boltzmann and non-Boltzmann excitation; number density ratios among electronic states are determined from QSS equations to calculate non-Boltzmann radiation, as shown later.

1. NO Spectra in 1994

The NO spectra obtained by Babikian et al. [2] are shown in Fig. 1. The present work calculates NO spectra under the Boltzmann distribution by using the temperatures measured by Babikian et al.: that is, $T = T_r = 560$, $T_v(\mathrm{NO}) = 950$, and $T_{\mathrm{ex}} = 11{,}500$ K, shown in Table 1. The calculated spectra are also presented in Fig. 1.

The presently calculated spectra consisting of NO γ, β, δ, and ε systems cannot explain the measured data as shown in the figure. In the measured spectra, the intensity of the $\gamma(0,0)$ is weaker than that of the $\gamma(0,1)$. But the intensity of $\gamma(0,0)$ is stronger than that of the $\gamma(0,1)$ in the calculated spectra. This is because the $\gamma(0,0)$ band is overlapped with the $\varepsilon(0,5)$ band. The intensities of the $\beta(0,5\text{–}7)$ bands in the calculated spectra are comparable with those of the $\gamma(0,4\text{–}6)$ bands; the spectra calculated by Babikian et al. [2] under the Boltzmann excitation also showed these $\beta(0,5\text{–}7)$ bands. But there is no trace of the β bands that are clearly seen in the calculated spectra.

In the present work, it was found that the spectra calculated with $T_e = 6100$ K under the Boltzmann, though not shown, also could not explain the measured spectra shown in the bottom of Fig. 1: temperature is too low to excite the NO $C^2\Pi_r$ state when the calculated intensities of NO γ band fit to those of the measured. The $\beta(0,5\text{–}7)$ bands are also clearly shown in the calculated spectra. It was also found that the measured spectra can be explained only when the β and ε radiations are completely excluded.

The presently calculated NO spectra are compared with those computed by a free radiation software named Specair [23]. For the convenience of comparison, a convolution-type slit function is selected in the Specair calculation. The spectra calculated by SPRADIAN07 and Specair, shown in the top of Fig. 1, are almost the same, even though there are discernible differences in line positions and intensities of the NO β. The difference of the line positions is believed to be due to the difference in calculating spin-orbit splitting for the ground electronic state of NO. The intensity differences may come from the differences in electronic-vibrational transition moments.

2. NO Spectra in 1998 and 1999

Figure 2 shows the spectra obtained by Park et al. [7] in 1998 (see Table 1). As mentioned, the relative intensities of the spectra [8] taken in 1998 are the same as those in 1999. Strong radiations mostly come from the NO δ and γ bands, and the bands of NO $\delta(0,2)$ and $\delta(0,3)$ among them are the most intense with the band origins at about 2055 and 2135 Å.

The spectra for NO γ, β, δ, and ε band systems are calculated under the Boltzmann with $T = T_r = 900$, $T_v(\mathrm{NO}) = 950$, and $T_e = 12{,}950$ K as shown in Fig. 2. The spectra calculated with the use of Specair [23] are also plotted for the comparison. The presently calculated spectra are significantly different from the measured spectra, as shown in the figure. The intensities of the $\varepsilon(0,2\text{–}4)$ bands are comparable with those of the $\delta(0,2\text{–}4)$ bands in the calculated spectra. The β bands start to appear at wavelengths longer than 2620 Å. But one cannot find such intense spectral bands, especially the ε bands, in the measured data. The calculated intensity of the $\gamma(0,0)$ appears higher than that of the measured intensity because it overlaps with the $\varepsilon(0,5)$ band.

The interesting feature is that spectral features with weak intensities can be seen in the measured data near the wavelengths of 2020 and 2100 Å. They are believed to be NO $\varepsilon(0,2)$ and $\varepsilon(0,3)$, because their band origins are presently calculated to be 2019.9 and 2097.0 Å, respectively. At first, we thought that the two peaks were from the highly excited vibrational states of NO γ or δ bands. But we

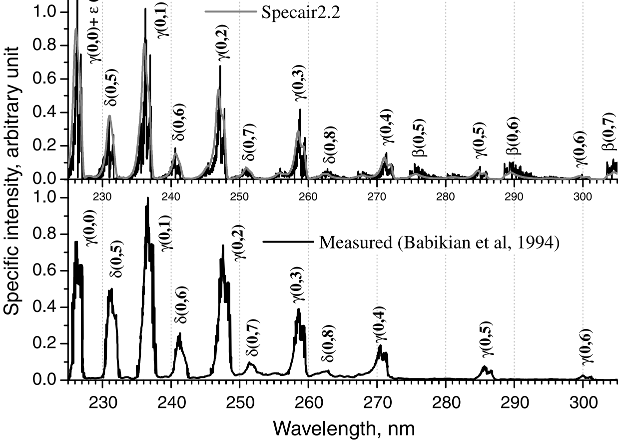

Fig. 1 Comparison of NO spectra calculated in the present work and obtained by Babikian et al. [2]: (top) the present spectra consisting of NO γ, β, δ, and ε band systems and (bottom) the measured spectra.

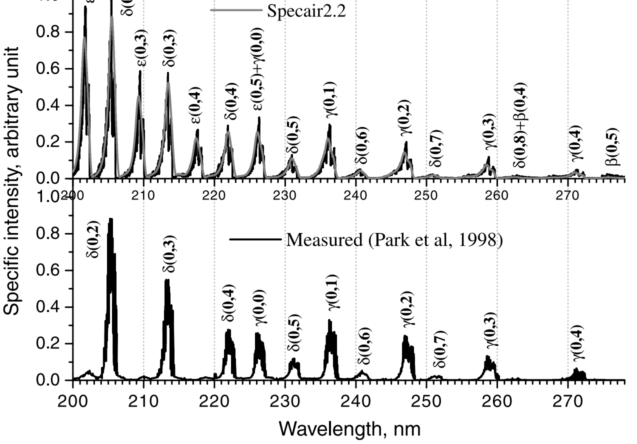

Fig. 2 Comparison of NO spectra calculated in the present work and obtained by Park et al. [7]: (top) the present spectra consisting of NO γ, β, δ, and ε band systems and (bottom) the measured spectra.

could not find any states that could produce the observed band origins and peaks.

3. Discrepancies

As mentioned previously and shown in Figs. 1 and 2, there are discrepancies between the experimental measurements and the theoretical computations. First, there are no NO β and only very weak ε band systems in the data obtained by Babikian et al. [2] and Park et al. [7,8]. Second, the electron temperature value of 6100 K determined by Babikian et al. [2] in the flow solution is very different from the electronic excitation temperature value of 11,500 K measured by Babikian et al. These phenomena cannot be explained by the existing theories on nonequilibrium radiation [15].

III. Interpretation of NO Spectra in Arcjet Flows

A. Literature Survey

To find an explanation to the two anomalies mentioned previously, the following inquires were made. Sharp and Rusch [24] observed airflow at wavelengths between 1900 and 2300 Å in the nighttime thermosphere of the Earth. Groth et al. [25] experimentally studied the reaction of ground state N and O atoms at a pressure of less than 5×10^{-2} torr in a laboratory. They obtained a synthetic spectrum consisting of NO γ, δ, and ε at the wavelengths of 1900 to 3400 Å and a spectrum from NO $C^2\Pi_r - A^2\Sigma^+$ transition at the wavelengths of 1.0 to 1.8 μm. In the spectra obtained by the two groups, intense spectra of NO $\gamma(v' = 0)$ and $\delta(v' = 0)$ were seen, but intensities of NO ε bands were much weaker. Sharp and Rusch [24] calculated the transition probability of the $C^2\Pi_r - A^2\Sigma^+$ to be about 5.6×10^6 s^{-1} for the $C^2\Pi_r - X^2\Pi_r$ transition probability of 2.1×10^7 s^{-1} under the assumption of absence of quenching of the $A^2\Sigma^+$. Groth et al. [25] also determined this transition probability to be 1.35×10^7 s^{-1} under the assumption that $C^2\Pi_r - X^2\Pi_r$ transition probability was 2.2×10^7 s^{-1}. The $C^2\Pi_r(v = 0)$ excitation phenomenon was called as NO chemiluminescence by Sharp and Rusch [24] and NO inverse predissociation by Groth et al. [25].

The spectra obtained by the two groups mentioned previously closely resemble those of Babikian et al. [2] and Park et al. [7,8]. The spectra of Groth et al. [25] and Park et al. [7,8] are compared in Fig. 3. The intensity of the NO $\delta(0,2)$ of Groth et al. [25] is only slightly lower, and the intensities of most of NO γ bands are only slightly higher than those of Park et al. [7,8]. The relative intensities of NO $\varepsilon(0,2\text{–}4)$ bands are very small, as mentioned. None of the NO β bands in the spectra obtained by Babikian et al. [2] can be found in the measured spectra of Groth et al. [25].

In the quenching experiment of Scheingraber and Vidal [26], a NO spectrum was measured after following the excitation of a $C^2\Pi_r(v = 0)$ state at a pressure of less than 0.1 torr. Though not shown, the spectrum showed intense NO γ and δ bands, which are also nearly close to the spectra obtained by Park et al. [7,8]. It indicates that the excited level only decays into the $X^2\Pi_r$ and the $A^2\Sigma^+(v = 0)$ states.

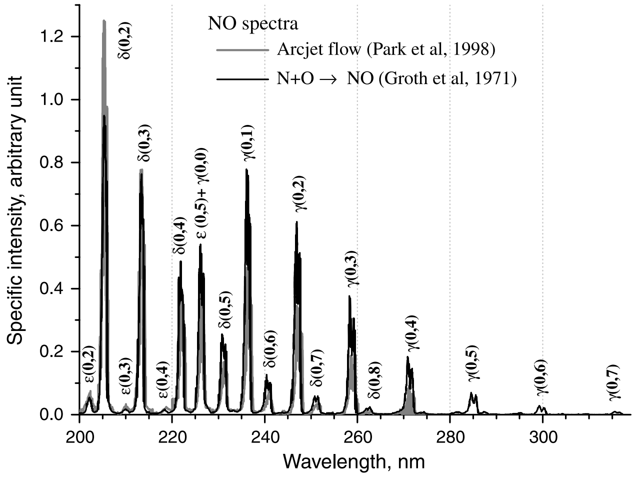

Fig. 3 Comparison of NO spectra measured by Park et al. [7] and Groth et al. [25].

Many studies [5,24,25,27–35] have been performed to understand populations of NO electronic states in recombination reaction of N and O atoms. For the recombination reaction of N and O atoms, excitations of NO electronic states and their generally accepted transitions [5,24,25,27–30,33–35] can be summarized as follows.

Group I:

$$\mathrm{N}\,(^4S) + \mathrm{O}(^3P) \rightleftharpoons \mathrm{NO}\,a^4\Pi \rightleftharpoons \mathrm{NO}\,C^2\Pi_r(v = 0) \tag{1}$$

$$\mathrm{NO}\ C^2\Pi_r(v = 0) \rightarrow \mathrm{NO}\,X^2\Pi_r + h\nu \qquad (\mathrm{NO}\,\delta)$$

Group II:

$$\mathrm{NO}\ C^2\Pi_r(v = 0) \rightarrow \mathrm{NO}\,A^2\Sigma^+ + h\nu \qquad (\mathrm{NO}\,C - A) \tag{2}$$

$$\mathrm{NO}\ C^2\Pi_r(v = 0) + M \rightarrow \mathrm{NO}\,A^2\Sigma^+ + M \tag{3}$$

$$\mathrm{NO}\ A^2\Sigma^+ \rightarrow \mathrm{NO}\,X^2\Pi_r + h\nu \qquad (\mathrm{NO}\,\gamma)$$

Group III:

$$\mathrm{NO}\ C^2\Pi_r(v = 0) + M \rightarrow \mathrm{NO}\,D^2\Sigma^+(v = 0) + M \tag{4}$$

$$\mathrm{NO}\ D^2\Sigma^+(v = 0) \rightarrow \mathrm{NO}\,X^2\Pi_r + h\nu \qquad (\mathrm{NO}\,\varepsilon)$$

Group IV:

$$\mathrm{N}\,(^4S) + \mathrm{O}(^3P) + M \rightarrow \mathrm{NO}\,a^4\Pi + M \tag{5}$$

$$\mathrm{NO}\ a^4\Pi + M \rightarrow \mathrm{NO}\,b^4\Sigma^- + M \qquad (\text{path } 1) \tag{6}$$

$$\mathrm{NO}\ a^4\Pi + M \rightarrow \mathrm{NO}\,B^2\Pi_r + M \qquad (\text{path } 2) \tag{7}$$

$$\mathrm{NO}\ b^4\Sigma^- + M \rightarrow \mathrm{NO}\,B^2\Pi_r + M \qquad (\text{path } 1) \tag{8}$$

$$\mathrm{NO}\ b^4\Sigma^- \rightarrow \mathrm{NO}\,a^4\Pi + h\nu \qquad (\mathrm{NO\ Ogawa}) \tag{9}$$

$$\mathrm{NO}\ B^2\Pi_r \rightarrow \mathrm{NO}\,X^2\Pi_r + h\nu \qquad (\mathrm{NO}\,\beta)$$

Here, M represents colliding particles, including electrons. In the present work, the excitation of the $D^2\Sigma^+(v = 0)$ state expressed in Eq. (4) is newly proposed.

Excitation rates for heavy-particle collisions K_h are expressed in SPRADIAN07 in the form

$$K_h(i, j) = A_h \left(\frac{T}{6000}\right)^n \exp\left(-\frac{T_d}{T}\right) \tag{10}$$

Here, A_h, n, and T_d are the excitation rate parameters. These values [10,13] contained in the code are shown in Table 3. Excitation rates for electron collisions (K_e) are calculated in the code using electron collision energies and their corresponding cross sections and Franck–Condon factors. The detailed values for available transitions are described elsewhere [9,13,15]. Predissociation, collisional, and

Table 3 Bound–bound electronic excitation rate parameters of NO by heavy-particle collisions [10,13]

	1–2, $X^2\Pi_r - a^4\Pi$			1–3, $X^2\Pi_r - A^2\Sigma^+$			2–4, $a^4\Pi - B^2\Pi_r$			4–5, $B^2\Pi_r - b^4\Sigma^-$		
M_h[a]	A_h[b]	n	T_d	A_h	n	T_d	A_h	n	T_d	A_h	n	T_d
N	4.15^{-10}	0.506	55,751	1.54^{-10}	0.496	62,912	1.94^{-10}	0.500	10,763	4.35^{-10}	0.499	3,850
O	5.75^{-10}	0.506	55,751	1.54^{-10}	0.496	62,912	1.94^{-10}	0.500	10,763	4.35^{-10}	0.499	3,850
N_2	1.23^{-15}	0.506	55,751	2.43^{-13}	0.496	62,913	1.38^{-11}	0.500	10,763	3.10^{-11}	0.499	3,850
O_2	7.86^{-11}	0.506	55,751	2.30^{-10}	0.496	62,912	4.08^{-10}	0.500	10,763	9.14^{-10}	0.499	3,850
NO	1.11^{-09}	0.506	55,751	3.47^{-10}	0.496	62,912	6.35^{-10}	0.500	10,763	1.42^{-09}	0.499	3,850

[a]Colliding heavy particle.
[b]$0.00^{-00} = 0.00 \times 10^{-00}$.

Table 4 Predissociation, collisional, and radiative transition rates

	Transition	Rate, s^{-1}	Ref. (year)
K_{prd}	$C^2\Pi_r(v=0, J>4.5) \rightarrow \mathrm{N}(^4S) + \mathrm{O}(^3P)$	$>3 \times 10^8$	[5] (1993)
K_h	$C^2\Pi_r \rightarrow D^2\Sigma^+$	Equation (18)	[5] (1993)
K_e	$C^2\Pi_r \rightarrow D^2\Sigma^+$	Equation (19)	[13] (2009)
A_r	$C^2\Pi_r \rightarrow X^2\Pi_r + A^2\Sigma^+$	3.3×10^7	[5] (1993)
A_r	$C^2\Pi_r \rightarrow A^2\Sigma^+$	$5.6 \pm 1.5 \times 10^6$	[24] (1981)
A_r	$C^2\Pi_r \rightarrow A^2\Sigma^+$	1.35×10^7	[25] (1971)
A_r[a]	$C^2\Pi_r \rightarrow A^2\Sigma^+$	9.57×10^6	[26] (1985)
A_r	$B^2\Pi_r \rightarrow X^2\Pi_r$	1.42×10^6	[13] (2009)
A_r	$A^2\Sigma^+(v=0) \rightarrow X^2\Pi_r$	5.08×10^6	[5] (1993)
A_r	$A^2\Sigma^+(v=0) \rightarrow X^2\Pi_r$	4.85×10^6	[36] (1999)
A_r	$C^2\Sigma^+(v=0) \rightarrow X^2\Pi_r$	2.01×10^7	[5] (1993)
A_r	$D^2\Sigma^+(v=0) \rightarrow X^2\Pi_r$	3.78×10^7	[5] (1993)
A_r	$D^2\Sigma^+(v=0) \rightarrow X^2\Pi_r$	4.08×10^7	[36] (1999)

[a]Deduced from the ratio $I(C,A) = (I(C,X) + I(C,A)) = 0.29$ and $A_r(C, X = A) = 3.3 \times 10^7$.

radiative transition rates not contained in SPRADIAN07 are found in literature, as shown in Table 4.

B. Population Mechanism of NO Electronic States

1. NO $C^2\Pi_r$ State

Equation (1) represents that the NO $C^2\Pi_r(v=0)$ state is populated by inverse predissociation. Inverse predissociation occurs as a result of level crossing in potential energy curves and a large transition probability between the crossing states. In Fig. 4, interaction potentials of NO electronic states are constructed in this work from the known spectroscopic constants [4,13], but those of the NO $a^4\Pi_r$ and $b^4\Sigma^-$ states are taken from the works of Scheingraber and Vidal [26] and Gadd and Slanger [33]. The energy level of the $C^2\Pi_r(v=0)$ is located very close to the dissociation limit [26,28,31–33,35,37,38] of the $X^2\Pi_r$. The $a^4\Pi$ state crosses the $C^2\Pi_r$ state at a point slightly above the $C^2\Pi_r(v=0)$ level. This suggests that the $C^2\Pi_r$ state is populated via the $a^4\Pi$ state by inverse predissociation, because the $X^2\Pi_r$ and $a^4\Pi$ states have the same electronic configuration in their dissociated states, as shown in Fig. 4. For this reason, the $a^4\Pi$ and $C^2\Pi_r$ states are likely to be in equilibrium with the ground electronic states of atoms $\mathrm{N}(^4S)$ and $\mathrm{O}(^3P)$.

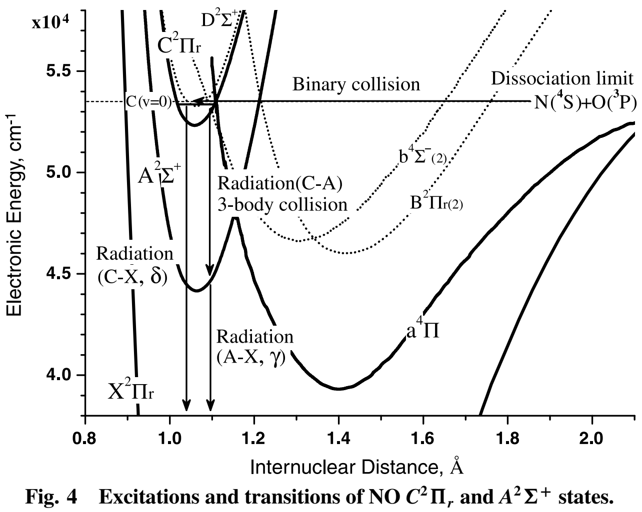

Fig. 4 Excitations and transitions of NO $C^2\Pi_r$ and $A^2\Sigma^+$ states.

Atoms N and O should be mostly in their ground states. First, there are large number of N and O atoms, as shown in Table 2. Such large number densities are possible at $T = 560$ K, because the flow is in thermochemical nonequilibrium. The hypothetical number density of NO in equilibrium with these N and O number densities at $T = 560$ K is 5.01×10^{64} cm^{-3}, which is much larger than $n_{\mathrm{NO}} = 2.41 \times 10^{13}$ cm^{-3} given in Table 2; if N and O atoms were equilibrated with a NO molecule, they cannot exist at $T = 560$ K, because they all recombine to form a NO molecule.

Second, distributions of electronic states of N and O atoms are computed with the use of SPRADIAN07 under both Boltzmann and non-Boltzmann excitations by using the values of Tables 1 and 2. The Boltzmann distributions of the atomic electronic states are calculated as

$$n_i = n_t \frac{Q_i}{Q_t} = n_t \frac{g_i \exp(-E_i/k_B T_e)}{\sum_i g_i \exp(-E_i/k_B T_e)} \tag{11}$$

The determined n_i are listed in Table 5. The non-Boltzmann distributions of electronic states are calculated by determining nonequilibrium factor κ_i [13–15]. Detailed procedures are described in [13–15]. The number densities due to non-Boltzmann excitation ($n_{i,nq}$) were determined by multiplying the n_i by the determined κ_i, as tabulated in Table 5. Thus, atoms N and O are mostly in their ground states of $\mathrm{N}(^4S)$ and $\mathrm{O}(^3P)$ under both the Boltzmann and non-Boltzmann distributions.

A master equation for the NO $C^2\Pi_r$ state for predissociation is expressed as

Table 5 Populations of atomic electronic states

Configuration	Term	g_i	E_i, cm^{-1}	n_i, cm^{-3}, %	κ_i	$n_{i,nq}$, cm^{-3}
Atom N						
$2s2.2p3$	$4S$	4	0.000	5.41×10^{15} (97.23)	1.00	5.41×10^{15}
$2s2.2p3$	$2D$	6	19,224.465	8.70×10^{13} (1.57)	1.00	8.70×10^{13}
$2s2.2p3$	$2D$	4	19,233.178	5.79×10^{13} (1.04)	1.00	5.79×10^{13}
$2s2.2p3$	$2P$	2	28,838.920	3.00×10^{12} (0.0540)	1.00	3.00×10^{12}
$2s2.2p3$	$2P$	4	28,839.307	6.00×10^{12} (0.108)	1.00	6.00×10^{12}
Atom O						
$2s2.2p4$	$3P$	5	0.000	1.52×10^{15} (55.82)	1.00	1.52×10^{15}
$2s2.2p4$	$3P$	3	158.265	8.77×10^{14} (32.27)	1.00	8.77×10^{14}
$2s2.2p4$	$3P$	1	226.977	2.88×10^{14} (10.58)	1.00	2.88×10^{14}
$2s2.2p4$	$1D$	5	15,867.862	3.60×10^{13} (1.32)	1.00	3.60×10^{13}
$2s2.2p4$	$1S$	1	33,792.582	1.05×10^{11} (0.00386)	$\sim$1.00	1.05×10^{11}
$2s2.2p3.(4S^*).3s$	$5S^*$	5	73,768.203	4.22×10^{07} ($\ll 1$)	0.0663	2.80×10^{06}

$$\frac{\partial n_C}{\partial t} = K_{\text{ivpr}} n_{\text{O}(X)} n_{\text{N}(X)} + \left[\sum_i K_h(i,C) n_h + \sum_i K_e(i,C) n_e + \sum_i A_r(i,C)\right] n_i - \left[K_{\text{prd}} + \sum_i K_h(C,i) n_h + \sum_i K_e(C,i) n_e + A_r(C, X/A)\right] n_C \tag{12}$$

where the X, A, and C stand for the states of NO $X^2\Pi_r$, $A^2\Sigma^+$, and $C^2\Pi_r$. The predissociation rate K_{prd} for the energy states higher than the $C^2\Pi_r(v = 0, J > 4.5)$ level is larger than 3×10^8 s^{-1} [5]. The values of $A_r(i, C)$ are presently not available. The term of $A_r(C, X/A)$ represents radiative decay rates from the $C^2\Pi_r$ state to both the $X^2\Pi_r$ and $A^2\Sigma^+$ states, and its value is about 3.3×10^7 s^{-1} [5].

Collisional transition rates by electron impacts and heavy-particle impacts were found to be much smaller than the radiative decay rate, as shown in the following subsections. When the detailed balances are applied as done by Laux [5], the master equation can be rewritten in the form of a QSS equation as

$$\frac{n_C}{n_{\text{eq},C}} = \frac{K_{\text{prd}}}{K_{\text{prd}} + A_r(C, X/A)} \tag{13}$$

Equation (13) approximately becomes 1, because the radiative decay rate is less than the predissociation rate by an order of magnitude. It indicates that the Boltzmann number density of the $C^2\Pi_r$ state is equal to that of the non-Boltzmann. Thus, the NO $C^2\Pi_r$ state is directly populated by inverse predissociation, and its state is nearly in equilibrium with the predissociation state [i.e., N(^4S) and O(^3P) atoms]. The transition from the $C^2\Pi_r$ to the $X^2\Pi_r$ is expected to result in intense NO δ radiation.

2. NO $A^2\Sigma^+$ State

The $A^2\Sigma^+$ state is populated by radiative decay of the $C^2\Pi_r(v = 0)$ state and collisions, as shown in Eqs. (2) and (3) and Fig. 4. The QSS equation for the NO $A^2\Sigma^+$ can be written as

$$\frac{n_A}{n_C} = \frac{K_h(C,A) n_h + K_e(C,A) n_e + A_r(C,A)}{K_h(A,X) n_h + K_e(A,X) n_e + A_r(A,X)} \tag{14}$$

As mentioned, the radiative transition from the $C^2\Pi_r$ to the $A^2\Sigma^+$ produced infrared spectrum [25,39]: the values of $A_r(C, A)$ are 5.6×10^6 s^{-1} [24] and 1.35×10^7 s^{-1} [25]. According to Sharp and Rusch [24], collisional transition [Eq. (3)] is not very effective to populate the $A^2\Sigma^+(v = 0)$ level. The states of $A^2\Sigma^+(v = 1, 2)$ are mostly populated by collisional excitations, but $v' = 1$ and 2 states were not seen in the obtained spectra of Babikian et al. [2] and Park et al. [7,8]. The K_e and K_h for the $C^2\Pi_r - A^2\Sigma^+$ transition are not taken into account in this work because they are presently not available. Thus, Eq. (14) implies that the radiative decay of the $C^2\Pi_r$ state is mostly responsible for the population of the $A^2\Sigma^+$ state.

The value of $A_r(A(v = 0), X)$ is about 4.97×10^6 s^{-1}, which is the average value of 5.08×10^6 [5] and 4.85×10^6 s^{-1} [36]. The transition rates K_h and K_e for the $A^2\Sigma^+ - X^2\Pi_r$ transition were estimated with the use of SPRADIAN07 for the conditions of flowfield data given in Tables 1 and 2. The calculated rates by electron impacts are $K_e(X, A) = 1.51 \times 10^{-15}$ and $K_e(A, X) = 1.65 \times 10^{-10}$ cm^3/s. The calculated average rates by N, O, N_2, O_2, and NO collisions are $K_h(X, A) = 5.98 \times 10^{-60}$ and $K_h(A, X) = 2.03 \times 10^{-10}$ cm^3/s. These two excitation rates are too small to excite NO electronic states from the ground state. The deexcitation rate $K_e(A, X) n_e$ is much less than $A_r(A, X)$. That of $K_h(A, X) n_h$ is 2.17×10^6 s^{-1}, which is comparable with $A_r(A(v = 0), X)$.

The number density ratios of the $A^2\Sigma^+(v = 0)$ to $C^2\Pi_r(v = 0)$ states are approximately calculated from Eq. (14):

$$\frac{n_{A(v=0)}}{n_{C(v=0)}} = \begin{cases} 0.784 & \text{when } A_r(C, A) = 5.60 \times 10^6 \text{ s}^{-1} \\ 1.89 & \text{when } A_r(C, A) = 1.35 \times 10^7 \text{ s}^{-1} \end{cases} \tag{15}$$

with $A_r(A(v = 0), X) = 4.97 \times 10^6$ s^{-1}, as mentioned. The total band intensity ratios become

$$\frac{I_{\text{NO},\gamma(v'=0)}}{I_{\text{NO},\delta(v'=0)}} = \frac{n_{A(v=0)} \cdot A_r(A(v = 0), X)}{n_{C(v=0)} \cdot A_r(C(v = 0), X)} = \begin{cases} 0.194 & \text{when } A_r(C, A) = 5.60 \times 10^6 \text{ s}^{-1} \\ 0.467 & \text{when } A_r(C, A) = 1.35 \times 10^7 \text{ s}^{-1} \end{cases} \tag{16}$$

Here, $A_r(C(v = 0), X)$ is 2.01×10^7 s^{-1} [5]. These ratios imply that the transition from $A^2\Sigma^+$ to $X^2\Pi_r$ causes strong NO γ radiation in addition to NO δ radiation.

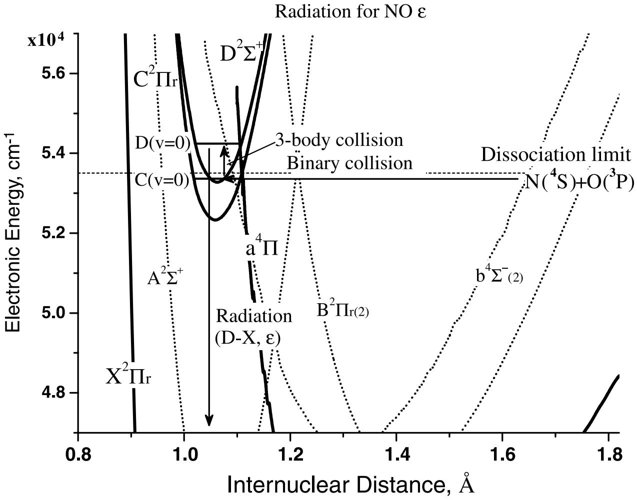

Fig. 5 Excitation and transition of NO $D^2\Sigma^+$ state.

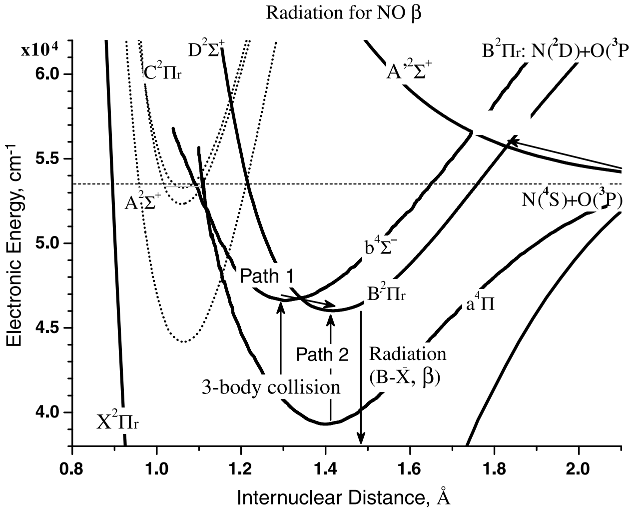

Fig. 6 Excitations and transition of NO $B^2\Pi_r$ state.

3. NO $D^2\Sigma^+$ State

The state of the NO $D^2\Sigma^+(v=0)$ was proposed to be excited from the $C^2\Pi_r(v=0)$ state by the collisional process, because the electronic term energy difference between the two states is only about 900 cm^{-1}. Even though the $a^4\Pi$ state crosses the $D^2\Sigma^+$ state, predissociation is not known to occur. Equation (4) and Fig. 5 describe such collisional excitation mechanisms of the $D^2\Sigma^+(v=0)$ state.

The QSS equation for the NO $D^2\Sigma^+$ can be written as

$$\frac{n_D}{n_C}=\frac{K_h(C,D)n_h+K_e(C,D)n_e}{A_r(D,X)} \tag{17}$$

The value of $A_r(D(v=0),X)$ is about 3.89×10^7 s^{-1}, which is the average value of 3.78×10^7 s^{-1} [5] and 4.08×10^7 s^{-1} [36]. The excitation rate $K_h(C,D)$ is not available in SPRADIAN07, but it was estimated by referring to the work of Laux [5] as

$$K_h(C,D)n_h=0.3\times10^{10}p\chi_h\sqrt{\frac{300}{T}}=1.39\times10^6\ \text{s}^{-1} \tag{18}$$

using the flow properties given by Babikian et al. [2]: that is, $T=560$ K, $p\simeq8.72\times10^{-4}$ atm, $\chi_h=0.724$, and $n_h=8.28\times10^{15}$ cm^{-3} (see Tables 1 and 2), where subscript h contains the N and O atoms. The excitation rate $K_e(C,D)$ was estimated as

$$K_e(C,D)=\sigma\times\sqrt{\frac{8k_BT_e}{\pi m_e}}\exp\left(-\frac{\Delta E(C,D)}{k_BT_e}\right)$$
$$=3.93\times10^{-8}\ \text{cm}^3/\text{s} \tag{19}$$

where cross section σ is assumed to be about 10^{-15} cm^2, and $\Delta E(C,D)$ is 900 cm^{-1}. The value of $K_e(C,D)n_e$ is 2.18×10^5 s^{-1}, which is consistent with the values estimated in SPRADIAN07, though not shown here. From these, it follows that

$$\frac{n_D(v=0)}{n_C(v=0)}=0.0412 \tag{20}$$

$$\frac{I_{\text{NO},\varepsilon(v'=0)}}{I_{\text{NO},\delta(v'=0)}}=\frac{n_D\cdot Ar(D(v=0),X)}{n_C\cdot Ar(C(v=0),X)}=0.0798 \tag{21}$$

Here, $A_r(C(v=0),X)$ is 2.01×10^7 s^{-1} [5]. Thus, total band intensity of the NO ε is weaker than those of the NO δ and γ band systems, as in the obtained spectra of Park et al. [7,8], Sharp and Rusch [24], and Groth [25].

4. NO $B^2\Pi_r$ State

As indicated in Eqs. (5–9), the excitation process for the NO $B^2\Pi_r$ state is more complicated than for other states, and its population is not related to inverse predissociation of the $C^2\Pi_r$ state. The possible excitation paths are shown in Fig. 6. Even though the $A'^2\Sigma^+$ state [40] crosses the $B^2\Pi_r$ state, predissociation is not known to occur. The $B^2\Pi_r$ state is populated only by three body collisions via the intermediate states $a^4\Pi$ produced through Eq. (5) and $b^4\Sigma^-$ produced through Eq. (6) ([27–30,33,34] and references therein).

Campbell and Mason [30], who measured the quenching rates of $B^2\Pi_r(v=0\text{–}3)$, showed that the $B^2\Pi_r(v=0,3)$ states are quenched more rapidly than the $B^2\Pi_r(v=1,2)$ levels. They mentioned that the intermediate state of the $b^4\Sigma^-$ plays significant roles in population of the $B^2\Pi_r$ levels by providing spin conservation, the degree of wave function overlap, and the modulus of energy defect. This is path 1 in Fig. 6 [Eqs. (5), (6), and (8)]. Path 2 in Fig. 6 [Eqs. (5) and (7)] is due to the perturbation of the specified levels of the $a^4\Pi$ state to allow spin-forbidden $a^4\Pi-B^2\Pi_r$ collision-induced transition. According to Ottinger and Vilesov [34], the $a^4\Pi(v=8,J=10.5)$ and $a^2\Pi(v=12,J=17.5)$ levels are in very close energy resonance with the $B^2\Pi_r(v=0,J=10.5)$ and $B^2\Pi_r(v=3,J=17.5)$ levels, respectively.

The master equation for the $B^2\Pi_r$ state can be written as

$$\begin{aligned}\frac{\partial n_B}{\partial t}&=K_h(a,B)n_an_h+K_h(b,B)n_bn_h+K_e(a,B)n_an_e\\&\quad+K_e(b,B)n_bn_e+\sum_i A_r(i,B)n_i\\&\quad-\Bigg[K_h(B,a)n_h+K_h(B,b)n_h+K_e(B,a)n_e\\&\quad+K_e(B,b)n_e+\sum_i A_r(B,i)\Bigg]n_B\end{aligned} \tag{22}$$

Here, a, b, and B represent the electronic states $a^4\Pi$, $b^4\Sigma^-$, and $B^2\Pi_r$. The excitation rates K_h, K_e, and $A_r(B,X)$ are estimated with the use of SPRADIAN07. They are $K_h(a,B)n_h=2.28\times10^{-3}$, $K_h(b,B)n_h=1.46\times10^6$, $K_e(a,B)n_e=4.86\times10^3$, $K_e(b,B)n_e=1.34\times10^4$ s^{-1}, and $A_r(B,X)=1.42\times10^6$ s^{-1}. The values of $A_r(i,B)$ are not available in the code. The values of $K_{e(h)}$ are much less than those for the transition between the $C^2\Pi_r$ and $D^2\Sigma^+$ states, except that of $K_h(b,B)n_h$. The population with the $K_h(b,B)n_h$ was expected to become small, because the $b^4\Sigma^-$ state is mostly populated from the $a^4\Pi$ state with $K_e(a,b)n_e=1.09\times10^4$ s^{-1} in SPRADIAN07. The intensities of NO β bands are expected to be much weaker than those of the NO ε bands because of relatively small collisional excitation rates and radiative transition probability. For these reasons, the NO β band system was not seen in the spectra obtained by Babikian et al. [2] and Park et al. [7,8].

C. Quasi-Steady-State Assumption

A QSS assumption has been known to be valid for the conditions of most experiments. Babikian et al. [2] and Park et al. [7,8] obtained spectra at different points from the nozzle exit in different years, as shown in Table 1. The fact that the three reported spectra have the same profiles indicates that the QSS assumption is valid for the arcjet experiments performed by them. The validity of the QSS assumption is examined for the electronic states of the NO molecule by introducing Δt as a time scale of change of conditions: Δt has an order of 10^{-4} s in the arcjet flows. More detailed descriptions can be found in [12,41].

As shown in the excitation mechanisms, the NO $A^2\Sigma^+$, $C^2\Pi_r$, and $D^2\Sigma^+$ states are satisfied with the QSS assumption, because the excitation rates and radiative decay rates have very large values compared with $1/\Delta t$. For the $B^2\Pi_r$ state, its radiative decay rates (which are the dominant terms in the sum of the outgoing rates) are much larger than the value of $1/\Delta t$. The leading terms in its incoming rates are written from Eq. (22) as

$$K_h(b,B)n_h\frac{n_b}{n_B} = 1.46\times 10^6\frac{n_b}{n_B}\ \mathrm{s}^{-1} \tag{23}$$

The ratio n_b/n_B was estimated to be not much different from 1, because the $B^2\Pi_r$ state populates through the $b^4\Sigma^-$ state, as shown in Eq. (8). Thus, the QSS assumption appears to be valid for the given conditions shown in Tables 1 and 2.

D. Electronic Temperatures

As shown in Eq. (13), the NO $C^2\Pi_r$ state is in equilibrium with the ground states of the N and O atoms. The $A^2\Sigma^+$ state is in a quasi-steady state between its outgoing rate and the incoming rate from the $C^2\Pi_r$, as shown in Eq. (14). The two states can be described by one electronic excitation temperature $T_{C,\mathrm{ex}}$. But the NO $B^2\Pi_r$ and $D^2\Sigma^+$ states are not equilibrated with the $C^2\Pi_r$ or $A^2\Sigma^+$ states. Their electronic temperatures become different from those of the $C^2\Pi_r$ or $A^2\Sigma^+$. Thus, electron temperature T_e cannot generally characterize the electronic states of the NO molecule, and it also does not have to be the same as electronic excitation temperatures T_{ex}.

From these facts, the electronic temperature for the NO $C^2\Pi_r$ and $A^2\Sigma^+$ states is estimated as

$$T_{C,\mathrm{ex}} = \frac{\Delta E(C,A)}{k_B\cdot \ln[(n_A/n_C)(g_C/g_A)]} \tag{24}$$

where $\Delta E(C,A)$ is 8210 cm^{-1} and g_C/g_A is 2. As shown in Eq. (15), the ratio n_A/n_C are 0.784 or 1.89 for $A_r(C,A) = 5.60\times 10^6$ [24] and $1.35\times 10^7\ \mathrm{s}^{-1}$ [25], respectively. Thus, the calculated electronic temperatures are 26,240 and 8880 K. The values of 11,500 and 12,950 K measured by Babikian et al. [2] and Park et al. [7,8] are between these two values. But the spectra calculated with $T = T_r = 560$ (or 900), $T_v(\mathrm{NO}) = 950$, and $T_{C,\mathrm{ex}} = 26,240$ K, though not shown here, are very different from the obtained spectra. The calculated spectra with $T_{C,\mathrm{ex}} = 8880$ K show that this temperature is slightly too low to explain the acquired spectra.

Scheingraber and Vidal [26] found the branching ratio $I(C,A)/(I(C,X)+I(C,A))$ to be about 0.29 in their quenching experiments. This ratio implies that $A_r(C,A)$ should be about $9.57\times 10^6\ \mathrm{s}^{-1}$ for the $A_r(C,X/A) = 3.3\times 10^7\ \mathrm{s}^{-1}$ [5]. This value is approximately equal to the average value of 5.60×10^6 [24] and $1.35\times 10^7\ \mathrm{s}^{-1}$ [25]. Thus, the electronic temperature $T_{C,\mathrm{ex}}$ for $A_r(C,A) = 9.57\times 10^6\ \mathrm{s}^{-1}$ becomes 11,980 K, which is very similar to the 11,500 and 12,950 K values measured by Babikian et al. [2] and Park et al. [7,8].

Figure 7 shows the spectra calculated with $T = T_r = 560$, $T_v(\mathrm{NO}) = 950$, and $T_{C,\mathrm{ex}} = 11,980$ K in this work. The electronic-vibrational number density ratio $n_{D(v=0)}/n_{C(v=0)}$ is calculated in the present work to be about 0.468 at $T_{C,\mathrm{ex}} = 11,980$ K under the Boltzmann distribution. The correct value of the ratio under the non-Boltzmann distribution calculated from Eq. (20) is 0.0412. The ratio between the values is 0.0881. To obtain the non-Boltzmann values of NO ε bands, their Boltzmann intensity values must be multiplied by 0.0881. The electronic excitation temperature of the NO $D^2\Sigma^+$ state (corresponding to the ratio 0.0412) is presently determined to be $T_{D,\mathrm{ex}} = 8680$ K. $T_{B,\mathrm{ex}}$ for the $B^2\Pi_r$ state is expected to be less than that of the $D^2\Sigma^+$ state, as mentioned earlier. In the calculation, $T_{B,\mathrm{ex}}$ was assumed to be 8680 K. The spectra calculated using these excitation temperatures are almost the same as the measured data, as presented in the figure.

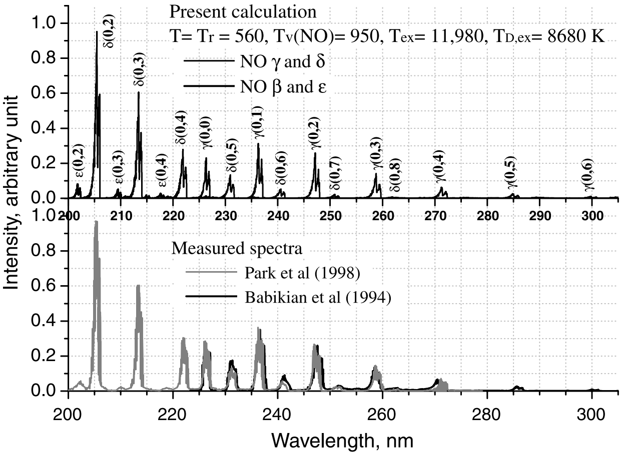

Fig. 7 Comparison of NO spectra calculated with $T_{\mathrm{ex}} = 11,980$ K and obtained by Babikian et al. [2] and Park et al. [7,8]: (top) the present spectra consisting of NO γ, β, δ, and ε band systems and (bottom) the measured spectra.

E. Uncertainties

When all $K_h(i,j)$ given in Table 3 are increased and decreased by a factor of 2, $T_{C,\mathrm{ex}}$ changes from 11,980 K given previously to 16,390 and 10,260 K, respectively. The 10,260 K value leads to the intensity ratios of NO δ to γ bands that are nearly the same as the measured values. However, the 16,390 K value leads to the ratios that are discernibly different from the measured values. Therefore, the K_h values in Table 3 are approximately the highest possible values that are compatible with the experimental data. This is partly expected: the rate parameter values for the $K_h(A,X)$ are deduced from the quenching rate data obtained at a temperature of up to 4000 K [10]. The $K_h(C,D)$ value expressed in Eq. (18) is from experiments also.

As mentioned earlier, the present work uses the radiative transition rates measured by Sharp and Rusch [24], Groth et al. [25], and Scheingraber and Vidal [26] for the NO $C^2\Pi_r$ to $A^2\Sigma^+$ transition. The value of Scheingraber and Vidal is the most recent and is approximately the average between the other two data values (see Table 4).

One-dimensional flowfield computation similar to that by Babikian et al. [2] was carried out along the center line of the nozzle in the present work with the use of a nozzle code named NOZ5T, originally developed by Park and Lee [1]. The calculated species number densities were not much different from those of Babikian et al. [2] shown in Table 2, except for O_2. The temperatures were calculated to be $T_e = T_v(N_2) = 3900$, $T_v(\mathrm{NO}) = 1120$, and $T = T_r = 820$ K instead of $T_e = 6100$, $T_v(N_2) = 3310$, $T_v(\mathrm{NO}) = 950$, and $T = T_r = 560$ K given by Babikian et al. [2]. $T_{C,\mathrm{ex}} = 10,640$ and $T_{D,\mathrm{ex}} = 7680$ K were obtained from Eq. (24) with $A_r(C,A) = 9.57\times 10^6\ \mathrm{s}^{-1}$ instead of $T_{C,\mathrm{ex}} = 11,980$ and $T_{D,\mathrm{ex}} = 8680$ K given previously. With all of these variations, the relative intensities of calculated spectra with these temperatures, though not shown here, were nearly the same as the calculated spectra shown in Fig. 7.

To determine the absolute intensities measured by Park et al. [7,8], at least two-dimensional flowfield computation must be performed, including the mixing phenomenon between the nozzle flow and the surrounding test-chamber flow. Because the conditions of the test chamber are not given in the works of Babikian et al. [2] and Park et al. [7,8], this calculation is presently not possible.

IV. Conclusions

The code SPRADIAN07 and its input data were used to estimate the collisional and radiative effects on the excitations of NO electronic states and to produce NO spectra. The excitation mechanisms for NO electronic states were qualitatively explained by introducing the models of inverse predissociation and collisional transitions. In the environments in which recombination of N and O atoms actively occur, such as at the conditions of the nozzle exit of arcjet flows, inverse predissociation directly populates the NO $C^2\Pi_r(v=0)$ state. The $C^2\Pi_r(v=0)$ state was found to be related to the intense emissions of NO δ and γ band systems. Collisional excitations are related to the emissions of NO ε and β, but their effects were found to be very small. Electronic excitation temperature for the NO $A^2\Sigma^+$ and $C^2\Pi_r$ states was determined to be about 11,980 K from the known radiative decay rates, and it was almost the same as the measured values. The spectra reproduced with the determined electronic temperature showed good agreement with the measured data.

References

[1] Park, C., and Lee, S. H., "Validation of Multitemperature Nozzle Flow Code," *Journal of Thermophysics and Heat Transfer*, Vol. 9, No. 1., Jan.–Mar. 1995, pp. 9–16.
doi:10.2514/3.622

[2] Babikian, D. S., Gopaul, N. K. J. L., and Park, C., "Measurement and Analysis of Nitric Oxide Radiation in an Arcjet flow," *Journal of Thermophysics and Heat Transfer*, Vol. 8, No. 4, Oct.–Dec. 1994, pp. 737–743.
doi:10.2514/3.606

[3] Abe, K., Kameyama, T., Kihara, H., Nishida, M., Ito, K., and Tanno, H., "Computational and Experiment of Nonequilibrium Nozzle Flow of Arc-heated Air," *Journal of Thermophysics and Heat Transfer*, Vol. 19, No. 4, Oct.–Dec. 2005, pp. 428–434.
doi:10.2514/1.13603

[4] "Nitric Oxide," *NIST Standard Reference Database Number 69* [online database], http://webbook.nist.gov/cgi/cbook.cgi?ID=C10102439&Units=SI [retrieved 20 Nov. 2008].

[5] Laux, C. O., "Optical Diagnostics and Radiative Emission of Air Plasmas," High Temperature Gasdynamics Lab., Stanford Univ., Rept. T-288, Stanford, CA, Aug. 1993.

[6] Rosen, B., *Donneés Spectroscopiques Relatives aux Molécules Diatomiques*, Pergamon, New York, 1970.

[7] Park, C. S., Newfield, M. E., Fletcher, D. G., Gökçen, T., and Sharma, S. P., "Spectroscopic Emission Measurements Within the Blunt-Body Shock Layer in an Arcjet Flow," *Journal of Thermophysics and Heat Transfer*, Vol. 12, No. 2, Apr.–June 1998, pp. 190–197.
doi:10.2514/2.6344

[8] Park, C. S., Newfield, M. E., Fletcher, D. G., and Gökçen, T., "Spectroscopic Measurements of Shock-Layer Flows in an Arcjet Facility," *Journal of Thermophysics and Heat Transfer*, Vol. 13, No. 1, Jan.–Mar. 1999, pp. 60–67.
doi:10.2514/2.6401

[9] Park, C., "Rate Parameters for Electronic Excitation of Diatomic Molecules 1: Electron-Impact Process," AIAA Paper 2008-1206, 2008.

[10] Park, C., "Rate Parameters for Electronic Excitation of Diatomic Molecules 2: Heavy Particle-Impact Phenomenon," AIAA Paper 2008-1446, 2008.

[11] Hyun, S. Y., Park, C., and Chang, K. S., "Rate Parameters for Electronic Excitation of Diatomic Molecules, III. CN Radiation Behind a Shock Wave," AIAA Paper 2008-1276, 2008.

[12] Hyun, S. Y., Park, C., and Chang, K. S., "Rate Parameters for Electronic Excitation of Diatomic Molecules: CN Radiation," *Journal of Thermophysics and Heat Transfer*, Vol. 23, No. 2, Apr.–June 2009, pp. 226–235.
doi:10.2514/1.36749

[13] Hyun, S. Y., "Radiation Code SPRADIAN07 and Its Applications," Ph.D. Thesis, Div. of Aerospace Engineering, School of Mechanical, Aerospace and Systems Engineering, Korea Advanced Inst. of Science and Technology, Daejeon, ROK, 2009.

[14] Hyun, S. Y., Park, C., Chang, K. S., Katsurayama, H., Fujita, K., and Abe, T., "User's Manual: Program SPRADIAN07 (Structured Package for Radiation Analysis 2007)," Div. of Aerospace Engineering, School of Mechanical, Aerospace and Systems Engineering, Korea Advanced Inst. of Science and Technology, Daejeon, ROK, 2007.

[15] Park, C., *Nonequilibrium Hypersonic Aerothermodynamics*, Wiley, New York, 1990.

[16] Park, C., "User's Manual: Nonequilibrium Air Radiation (NEQAIR) Program," NASA TM86707, July 1985.

[17] Laux, C. O., and Knucinnt, C. H., "Arrays of Radiative Transition Probabilities for the N_2 First and Second Positive, NO Beta and Gamma, N_2^+ First Negative, and O_2 Schumann-Runge Band Systems," *Journal of Quantitative Spectroscopy and Radiative Transfer*, Vol. 48, No. 1, 1992, pp. 9–24.
doi:10.1016/0022-4073(92)90003-M

[18] Kovács, I., *Rotational Structure in the Spectra of Diatomic Molecules*, Adam Hilger, London, 1969.

[19] Whiting, E. E., Paterson, J. A., Kovács, I., and Nicholls, R. W., "Computer Checking of Rotational Line Intensity Factors for Diatomic Transitions," *Journal of Molecular Spectroscopy*, Vol. 47, No. 1, July 1973, pp. 84–98.
doi:10.1016/0022-2852(73)90078-7

[20] Whiting, E. E., and Nicholls, R. W., "Reinvestigation of Rotational-Line Intensity Factors in Diatomic Spectra," *Astrophysical Journal Supplement Series*, Vol. 27, No. 235, 1974, pp. 1–19.
doi:10.1086/190286

[21] Whiting, E. E., Schadee, A., Tatum, J. B., Hougen J. T., and Nicholls, R. W., "Recommended Conventions for Defining Transition Moments and Intensity Factors in Diatomic Molecular Spectra," *Journal of Molecular Spectroscopy*, Vol. 80, No. 2, Apr. 1980, pp. 249–256.
doi:10.1016/0022-2852(80)90137-X

[22] Mulliken, R. S., and Christy, A., "Λ-Type Doubling and Electron Configurations in Diatomic Molecules," *Physical Review*, Vol. 38, No. 1, July 1931, pp. 87–119.
doi:10.1103/PhysRev.38.87

[23] Specair, Software Package, Ver. 2.2.0.0, Lab. d'Énergétique Moléculaire, Macroscopique et Combustion, École Centrale Paris, Paris, www.specair-radiation.net [retrieved 16 Oct. 2008].

[24] Sharp, W. E., and Rusch, D. W., "Chemiluminescence of Nitric Oxide: the NO ($C^2\Pi - A^2\Sigma^+$) Rate Constant," *Journal of Quantitative Spectroscopy and Radiative Transfer*, Vol. 25, No. 5, May 1981, pp. 413–417.
doi:10.1016/0022-4073(81)90059-5

[25] Groth, W., Kley, D., and Schurath, U., "Rate Constant for the Infrared Emission of the NO ($C^2\Pi - A^2\Sigma^+$) Transition," *Journal of Quantitative Spectroscopy and Radiative Transfer*, Vol. 11, No. 10, Oct. 1971, pp. 1475–1480.
doi:10.1016/0022-4073(71)90109-9

[26] Scheingraber, H., and Vidal, C. R., "Fluorescence Spectroscopy and Franck-Condon-Factor Measurements of Low-Lying NO Rydberg states," *Journal of the Optical Society of America B (Optical Physics)*, Vol. 2, No. 2, Feb. 1985, pp. 343–354.
doi:10.1364/JOSAB.2.000343

[27] Young, R. A., and Sharpless, R. L., "Chemiluminescent Reactions Involving Atomic Oxygen and Nitrogen," *Journal of Chemical Physics*, Vol. 39, No. 4, Mar. 1963, pp. 1071–1102.
doi:10.1063/1.1734361

[28] Gross, R. R., and Cohen, N., "Temperature Dependence of Chemiluminescent Reactions. 2: Nitric Oxide Afterglow," *Journal of Chemical Physics*, Vol. 48, No. 6, Mar. 1968, pp. 2582–2588.
doi:10.1063/1.1669486

[29] Campbell, I. M., and Neal, S. B., "New Observation on Nitric Oxide β Band Chemiluminescence," *Chemical Physics Letters*, Vol. 8, No. 6, Mar. 1971, pp. 612–1971.
doi:10.1016/0009-2614(71)80107-0

[30] Campbell, I. M., and Mason, R. S., "The Location of NO ($b^4\Sigma^-$) and the Excitation Mechanism of NO β Bands," *Journal of Photochemistry*, Vol. 8, No. 5, June 1978, pp. 375–389.

[31] Rottke, H., and Zacharias, H., "PhotoIonization of Single Rotational Levels in Excited $B^2\Pi$, $C^2\Pi$, and $D^2\Sigma^+$ states of $^{14}N^{16}O$," *Journal of Chemical Physics*, Vol. 83, No. 10, Nov. 1985, pp. 4831–4844.
doi:10.1063/1.449744

[32] Tshukiyama, K., Munakata, T., Tsukakoshi, M., and Kasuya, T., "Fluorescence Lifetimes of NO $A^2\Sigma^+(v' = 3$ and $4)$, $C^2\Pi(v' = 0)$, and $D^2\Sigma^+(v' = 0)$ Studied by Tunable VUV Laser Excitation," *Chemical Physics*, Vol. 121, No. 1, Mar. 1988, pp. 55–62.
doi:10.1016/0301-0104(88)87004-6

[33] Gadd, G. E., and Slanger, T. G., "NO($B^2\Pi$) Radiative Lifetimes: $v = 0$–6," *Journal of Chemical Physics*, Vol. 92, No. 4, Feb. 1990, pp. 2194–2202.
doi:10.1063/1.458011

[34] Ottinger, C., and Vilesov, A. F., "Intramolecular Collisional Transfer In No ($a^4\Pi \rightarrow B^2\Pi$, $b^4\Sigma^-$): Gateway-Type, Resonant Versus Direct, Nonresonant Mechanisms," *Journal of Chemical Physics*, Vol. 100, No. 3, Feb. 1994, pp. 1805–1814.
doi:10.1063/1.466533

[35] Matveev, A. A., Pravilov, A. M., and Vilesov, A. F., "Anomalously Large Isotope Effect in the Chemiluminescence from $N(^4S) + O(^3P)$ Recombination," *Chemical Physics Letters*, Vol. 217, No. 5–6, Jan. 1994, pp. 582–588.
doi:10.1016/0009-2614(93)E1432-G

[36] Luque, J., and Crosley, D. R., "Transition Probabilities and Electronic Transition Moments of the $A^2\Sigma^+ - X^2\Pi$ and $D^2\Sigma^+ - X^2\Pi$ Systems of Nitric Oxide," *Journal of Chemical Physics*, Vol. 111, No. 16, Oct. 1999, pp. 7405–7415.
doi:10.1063/1.480064

[37] Copeland, R. A., Dyer, M. J., Bloemink, H. I., and Slanger, T. G., "The NO($a^4\Pi$) State: Collisional Removal of $v = 11$ and $a^4\Pi - B^2\Pi$ Interactions," *Journal of Chemical Physics*, Vol. 107, No. 7, Aug. 1997, pp. 2257–2266.
doi:10.1063/1.474603

[38] Luque, J., and Crosley, D. R.,"Collisional Energy Transfer of NO $D^2\Sigma^+(v' = 0)$ and $A^2\Sigma^+(v' = 4)$ by O_2, N_2, Ar, and NO," *Journal of Physical Chemistry A*, Vol. 104, No. 12, Mar. 2000, pp. 2567–2572.
doi:10.1021/jp993159a

[39] Dingle, T. W., Freedman, P. A., Gelernt, B., Jones, W. J., and Smith, W. M., "NO ($C^2\Pi - A^2\Sigma^+$) Emission During the Radiative Recombina-

tion of N and O Atoms," *Chemical Physics*, Vol. 8, No. 1–2, Apr. 1975, pp. 171–177.
doi:10.1016/0301-0104(75)80104-2

[40] Sun, H., and Nakamura, H., "Theoretical Study of the Dissociative Recombination of NO^+ with Slow Electrons" *Journal of Chemical Physics*, Vol. 93, No. 9, Nov. 1990, pp. 6491–6501.
doi:10.1063/1.458966

[41] Park, C., "Spectral Line Intensities in a Nonequilibrium Nitrogen Plasma," *Journal of Quantitative Spectroscopy and Radiative Transfer*, Vol. 8, No. 10, Oct. 1968, pp. 1633–1653.
doi:10.1016/0022-4073(68)90107-6